OXFORD

ORIGINAL ARTICLE

# DNA Methyltransferase 3A Is Involved in the Sustained Effects of Chronic Stress on Synaptic Functions and Behaviors

Jing Wei[1], Jia Cheng[1], Nicholas J. Waddell[2], Zi-Jun Wang[1], Xiaodong Pang[3], Qing Cao[1], Aiyi Liu[1], Javed M. Chitaman[2,4], Kristen Abreu[2], Rahul Singh Jasrotia[2], Lara J. Duffney[1], Jinfeng Zhang[3], David M. Dietz[5], Jian Feng[2,4] and Zhen Yan[1]

[1]Department of Physiology and Biophysics, School of Medicine and Biomedical Sciences, State University of New York at Buffalo, Buffalo, NY 14203, USA, [2]Department of Biological Science, Florida State University, Tallahassee, FL 32306, USA, [3]Department of Statistics, Florida State University, Tallahassee, FL 32306, USA, [4]Program in Neuroscience, Florida State University, Tallahassee, FL 32306, USA and [5]Department of Pharmacology and Toxicology, State University of New York at Buffalo, Buffalo, NY 14203, USA

Address correspondence to Zhen Yan, Email: zhenyan@buffalo.edu or Jian Feng, Email: feng@bio.fsu.edu.

## Abstract

Emerging evidence suggests that epigenetic mechanisms regulate aberrant gene transcription in stress-associated mental disorders. However, it remains to be elucidated about the role of DNA methylation and its catalyzing enzymes, DNA methyltransferases (DNMTs), in this process. Here, we found that male rats exposed to chronic (2-week) unpredictable stress exhibited a substantial reduction of *Dnmt3a* after stress cessation in the prefrontal cortex (PFC), a key target region of stress. Treatment of unstressed control rats with DNMT inhibitors recapitulated the effect of chronic unpredictable stress on decreased AMPAR expression and function in PFC. In contrast, overexpression of *Dnmt3a* in PFC of stressed animals prevented the loss of glutamatergic responses. Moreover, the stress-induced behavioral abnormalities, including the impaired recognition memory, heightened aggression, and hyperlocomotion, were partially attenuated by *Dnmt3a* expression in PFC of stressed animals. Finally, we found that there were genome-wide DNA methylation changes and transcriptome alterations in PFC of stressed rats, both of which were enriched at several neural pathways, including glutamatergic synapse and microtubule-associated protein kinase signaling. These results have therefore recognized the potential role of DNA epigenetic modification in stress-induced disturbance of synaptic functions and cognitive and emotional processes.

**Key words:** DNA methylation, epigenetics, glutamatergic synapse, prefrontal cortex, stress

## Introduction

It is well known that prolonged stress could trigger maladaptive responses, which is associated with the precipitation of mental disorders, including anxiety, depression, post-traumatic stress disorder (PTSD), and schizophrenia (Gispen-de Wied 2000; Smith et al. 2004; de Kloet et al. 2005; Mineur et al. 2006). The prefrontal cortex (PFC), a brain region critical for high-level executive functions, such as working memory, decision-making, and emotional control (D'Esposito et al. 1995; Rainer et al. 1998; Miller and Cohen 2001), is a key target of stress (Radley et al. 2006; Arnsten 2009; McEwen and Morrison 2013). Glutamatergic transmission mediated by PFC pyramidal neurons, which is particularly important for PFC-dependent functions (Goldman-Rakic 1995), has been found to be highly sensitive to stress (Popoli et al. 2011; Yuen et al. 2012; Wei et al. 2014).

The sustained impact of chronic stress on cognitive and emotional behaviors suggests that aberrant gene expression may occur after stress (Bagot et al. 2016). Emerging evidence indicates that altered epigenetic regulation of gene transcription, such as histone modifications and DNA methylation, plays an important role in stress responses (Sultan and Day 2011; Stankiewicz et al. 2013; Klengel et al. 2014; Vinkers et al. 2015; Wei et al. 2016). DNA methylation, a process by which methyl groups are covalently coupled to the DNA molecule, typically acts to repress gene transcription when located at a gene promoter. The conversion of cytosine bases to 5-methylcytosine is catalyzed by DNA methyltransferases (DNMTs). Notably, abnormal DNA methylation of many genes, such as *BDNF*, FK506-Binding Protein 5 (*FKBP5*), Catechol-O-methyltransferase (*COMT*) and Spermidine/spermine N1-acetyl-transferase (*SAT1*), was found in the brain or blood samples from patients with PTSD or major depressive disorder or suicide subjects (Fiori and Turecki 2011; Ursini et al. 2011; Kang et al. 2013; Klengel et al. 2013). In addition, the promoter hypermethylation of serotonin transporter gene *SLC6A4* or glucocorticoid receptor (GR) gene *NR3C1* has been observed in human subjects with childhood traumatic experience or major depressive disorder (McGowan et al. 2009; Kim et al. 2013; Steiger et al. 2013; Wankerl et al. 2014). Animal studies also demonstrated that DNA methylation enzymes and DNA methylation are correlated with stress-related disorders (LaPlant et al. 2010; Labonté et al. 2012; Elliott et al. 2016; Feng et al. 2017).

Given the link between DNA methylation and stress-associated mental disorders in human studies, we sought to decipher out the role of DNA methylation in the sustained changes at PFC synapses and PFC-dependent behaviors induced by chronic unpredictable stress. We used peripubertal rats in this study, because the adolescent brain is more sensitive to stressors due to the dramatic hormonal and neurodevelopmental changes around puberty (Paus et al. 2008; Lupien et al. 2009). Moreover, human studies have discovered that early adversity during critical periods is strongly associated with developing abnormal behaviors and psychiatric disorders (Heim and Nemeroff 2001; Toth et al. 2008; Márquez et al. 2013; Niwa et al. 2013; Haller et al. 2014).

## Materials and Methods

### Chronic Unpredictable Stress Paradigm

All experiments were performed with the approval of the Institutional Animal Care and Use Committee of the State University of New York at Buffalo. Male Sprague Dawley rats were weaned at 21 days old and randomly assigned to the control (stress-naïve) or stress group. Animals were group housed for both groups. For the chronic unpredictable stress, animals (starting at 3 weeks old) were exposed to 2 unpredictable stressors each day for 14 days. The unpredictable stressors were randomly chosen from 4 choices, including restraint in an air-assessable cylinder (4 h), forced swim in cold water (15 °C, 5 min), elevated platform (30 min), and tilted mouse cage with wet bedding on orbital shaking (45° angle, 100 cycle/min, 1 h). The arrangement of stressors was changed every day in order to avoid habituation. All animals were group housed (2–4 rats per cage) with the standard light/dark cycle, and control versus stressed groups were housed separately. Behavioral testing, electrophysiological experiments, and samples collection for quantitative real-time reverse transcription-polymerase chain reaction (RT-PCR) and western blotting were performed at 5–7 days after stress cessation.

### Animal Surgery

In vivo delivery of compounds or viruses was achieved by stereotaxic injection bilaterally into medial PFC of 5-week-old rats with a Hamilton syringe (needle gauge 31) as we described previously (Yuen et al. 2012; Wei et al. 2014). RG108 (2 µL, 100 µM) or vehicle (5% hydroxypropyl $\beta$-cyclodextrin) injection to control rats was performed 2–3 days before the electrophysiological experiments and behavioral testing. Bicistronic p1005+ HSV vectors, in which *GFP* is driven by CMV promoter and *Dnmt3a* is driven by IE4/5 promoter, were generated as previously described (LaPlant et al. 2010). Mouse cDNA was used for the original cloning of the *Dnmt3a* plasmid (Linhart et al. 2007). HSV (1 µL, *GFP* or *Dnmt3a*) injection was performed in the next day after stress cessation. Electrophysiological experiments and behavioral testing were performed 3 days after surgery.

### Behavioral Testing

All behavioral experiments were performed at late afternoon and early evening. All the subjects were moved to the testing room illuminated with constant dim lights at least 1 h before the task started. The novelty-suppressed feeding test was performed at bright light. All the behavioral tests were manually scored by experimenters who were blind to the treatments that animals received.

Temporal order recognition (TOR) task was conducted as we previously described (Yuen et al. 2012; Wei et al. 2014). All objects were affixed to a round platform (diameter: 61.4 cm). Objects were Lego blocks with similar sizes but different shapes and colors. Each rat was habituated twice on the platform (without objects) for 5 min on the day of behavioral experiments. This task comprised 2 sample phases and 1 test trial. In each sample phase, the animals were allowed to explore 2 identical objects for 3 min. Different objects were used for sample phases I and II, with a 1-h delay between the sample phases. The test trial (3 min) was given 3 h after sample phase II. During the test trial, an object from sample phase I and an object from sample phase II (distance: ~20 cm) were used. The positions of 2 objects were counterbalanced between the animals. If TOR memory is intact, the animals will spend more time exploring the object from sample I (i.e., the novel object presented less recently) in the test trial. The time animal spent sniffing the object at its proximity

was calculated as object exploration time. A discrimination ratio (DR), the proportion of time spent exploring the novel versus the familiar object during the test trial, was calculated (the difference in time spent exploring the novel and familiar objects divided by the total time spent exploring both objects).

Resident–intruder (RI) tests used a protocol (Veenema et al. 2006; Márquez et al. 2013) with some modifications. Briefly, each rat was single housed for 24 h before the RI test. Then, the resident rat was exposed to an intruder, which was a slightly smaller (5–15% lighter) unfamiliar SD rat (male), in its home cage for 10 min. The attack of the resident rat with the intruder was scored to measure aggression-related behaviors, including the attack latency time, number of attacks, lateral threat, clinch, offensive upright, and keep down. The latter 4 parameters were summarized as total aggressive behavior.

Locomotion tests measured the number of crossing a midline in an empty cage within 5 min.

Open-field tests used an open rectangular arena ($60 \times 80$ cm) with opaque wall. The amount of time that the animal spent in the center area ($25 \times 25$ cm) and the number of entries into the center within 10 min were counted.

Elevated plus maze test used an apparatus (height from floor: 45 cm) consisting of 2 open arms (arm width: 7.5 cm; arm length: 40 cm) and 2 closed arms (arm width: 7.5 cm; arm length: 40 cm; wall height: 27.6 cm). The rat was placed at the junction of the 4 arms of the maze, facing an open arm. Each rat was left on the elevated plus maze for 5 min. An entry was counted only if all 4 paws were inside the arm. The number of entries into open arms and the time spent in open arms were recorded (Qin et al. 2016).

Light–dark box test used a box ($35 \times 26 \times 34$ cm) divided into 2 identical chambers, a dark chamber completely covered by black acrylic sheet and a light chamber illuminated by bright overhead lighting. There was a door ($7.6 \times 12.7$ cm) connecting the 2 chambers and allowing the animal to move freely. The rat was placed in the light compartment before the 10-min test session started. The time spent in the light chamber and the number of entries into the light chamber were counted.

Novelty-suppressed feeding test was used to measure stress-induced anxiety-like behaviors. Before the test, animals were food deprived for 24 h with free access to water. One food pellet was placed on a round white platform (diameter: 10 cm) that was attached to the center of an arena ($60 \times 80$ cm). The rat was first placed in a corner of the arena. The latencies of the first approach and the first bite of the food pellet during the 10-min test session were recorded (Stedenfeld et al. 2011).

Social approach test was used to measure the sociability. The animal was first habituated in an apparatus ($70 \times 50 \times 50$ cm) containing a capsule for 10 min and then was returned to the home cage. The apparatus was cleaned and a social stimulus (an age- and sex-matched rat) was placed inside the capsule. The test animal was put back into the apparatus to explore for 10 min. The time spent on interacting with the social stimulus was measured.

Sucrose preference test was used to measure anhedonia. Each rat was single housed for 24 h before the test. During the test day, the animal was first deprived of water for 4 h and then had free choice of drinking either 0.5% sucrose solution (w/v) or plain water for 3 h. The positions of 2 bottles were counterbalanced across the left and right. Each fluid consumption was measured and the sucrose preference ratio was calculated as a percentage of the volume of sucrose intake over the total volume of fluid intake (Duric et al. 2010).

## Quantitative Real-Time RT-PCR

To compare the mRNA levels, quantitative RT-PCR was used. Total RNA was isolated from rat PFC punches using TRIzol reagent (Invitrogen) and treated with DNase I (Invitrogen) to remove genomic DNA. Then, SuperScript III first-strand synthesis system for RT-PCR (Invitrogen) was used to obtain cDNA from the tissue mRNA, followed by treatment with RNase H (2 U/L) for 20 min at 37 °C. Quantitative real-time RT-PCR was performed using the iCycler iQ Real-Time PCR Detection System and iQ Supermix (Bio-Rad) according to the manufacturer's instructions. In brief, GAPDH was used as the housekeeping gene for quantitation of the expression of target genes in samples from control versus stressed rats. Fold changes in the target gene relative to the GAPDH endogenous control gene was determined by: Fold change $= 2^{-\Delta(\Delta C_T)}$, where $\Delta C_T = C_{T,target} - C_{T,GAPDH}$, and $\Delta(\Delta C_T) = \Delta C_{T,stressed} - \Delta C_{T,control}$. $C_T$ (threshold cycle) is defined as the fractional cycle number at which the fluorescence reaches $10\times$ the standard deviation of the baseline. A total reaction mixture of 25 µL was amplified in a 96-well thin-wall PCR plate (Bio-Rad) using the following PCR cycling parameters: 95 °C for 5 min followed by 40 cycles of 95 °C for 30 s, 55 °C or 60 °C for 30 s, and 72 °C for 60 s. Primer sequences are listed below. *Dnmt1*: (forward) AGCAAGGTCAAGGTCATCTA; (reverse) GGCATTTCTTTTTGTCTCAG. *Dnmt3a*: (forward) ATCTACGAAGTCCTCCAGGT; (reverse) ACATGTCGGTGTAAACTTCC. *Dnmt3b*: (forward) TCTGATGTCACTAACAACAA; (reverse) GTGCAGTAGGACTGATAGCC. *Tet1*: (forward) TCACCAGAGGATCTTGGTGCTA; (reverse) GCAGCTATTACCAGAGGTACTG. *Tet2*: (forward) GGAGGGATAAAACGCACAGTCA; (reverse) GTTCCGTGTTGGGAAAGCATCT. *Tet3*: (forward) AGTTGATGGACCTGTTCCAGGT; (reverse) GACTCATCTCACGGTTGAAGGT. *Gria1*: (forward) AGGGGTCCGCCCTGAGAAAT; (reverse) CTTGTCCTTGGAGTCACCTC. *Gria2*: (forward) AAGGATCCTCATTAGGAACC; (reverse) CAACGTTGCTCAGACTGAGG. *Hdac7*: (forward) GAGCAAGAACTTCGGCAACT; (reverse) CCAAGGGCTCAAGAGTTCTG. *Zfp423*: (forward) CCCATGACCTGTGTGTTCAG; (reverse) TTGACTTGTCACGCTGTTCC. *Grid1*: (forward) CACAGGAAGGCTACCTCCAA; (reverse) TGAGCTGTCTTCCCGAAACT. *Grid2*: (forward) CCAGGAGCAACAGAAACGAT; (reverse) CACCTTTTTGAAGGGCAACAT. *Gapdh*: (forward) GACAACTCCCTCAAGATTGTCAG; (reverse) ATGGCATGGACTGTGGTCATGAG. Quantitative real-time RT-PCR was performed in triple reactions.

## Electrophysiological Recordings

Whole-cell patch-clamp experiments were performed with a Multiclamp 700A amplifier and Digidata1322A data acquisition system (Molecular Devices, Sunnyvale, CA). PFC-containing slices were positioned in a perfusion chamber attached to the fixed stage of an upright microscope (Olympus, Center Valley, PA) and submerged in continuously flowing oxygenated artificial cerebrospinal fluid (ACSF) (in mM: 130 NaCl, 26 NaHCO$_3$, 3 KCl, 5 MgCl$_2$, 1.25 NaH$_2$PO$_4$, 1 CaCl$_2$, 10 Glucose, pH 7.4, and 300 mOsm). Neurons were visualized with the infrared differential interference contrast video microscopy. For AMPAR-EPSC recordings, bicuculline (10 µM) and D-APV (25 µM) were added in ACSF, and the patch electrodes contained internal solution (in mM): 130 Cs-methanesulfonate, 10 CsCl, 4 NaCl, 10 HEPES, 1 MgCl$_2$, 5 EGTA, 2.2 QX-314, 12 phosphocreatine, 5 ATP, 0.2 GTP, 0.1 leupeptin, pH 7.2–7.3, and 265–270 mOsm. For GABA$_A$R-mediated inhibitory postsynaptic current (GABA$_A$R-IPSC), D-APV (25 µM) and CNQX (25 µM) were added in ACSF,

and the internal solution contained (in mM): 100 CsCl, 30 N-methyl-D-glucamine (NMG), 10 HEPES, 4 NaCl, 1 MgCl$_2$ 5 EGTA, 2.2 QX-314, 12 phosphocreatine, 5 MgATP, 0.5 Na$_2$GTP, pH 7.2–7.3, and 265–270 mosM. Evoked excitatory postsynaptic current (EPSC) or IPSC was generated with a pulse from a stimulation isolation unit controlled by a S48 pulse generator (Grass Technologies, West Warwick, RI). A bipolar stimulating electrode (FHC, Bowdoinham, ME) was placed approximately 100 μm from the neuron under recording. Tight seals (2–10 GΩ) were obtained by applying negative pressure. The membrane was disrupted with additional suction, and the whole-cell configuration was obtained. Membrane potential was maintained at −70 mV for recordings. To obtain the input–output responses, EPSC or IPSC was elicited by a series of stimulation intensities with the same duration of pulses. Electrophysiological recording was performed on layer V pyramidal neurons in prelimbic area. Recordings from control versus stressed animals were interleaved throughout the course of all experiments.

## Western Blotting

Prelimbic cortex from rat brain slices was collected for total protein and nuclear fraction process. For total protein extraction, samples were homogenized in 1% SDS lysis buffer and followed by centrifugation at 14 000×$g$ for 15 min. After centrifugation, the supernatant fraction was collected, boiled in 2× SDS loading buffer for 5 min, and then separated on 7.5% SDS-polyacrylamide gels. Nuclear fraction extractions were processed according to the manufacturer's instructions (Life Technologies). Briefly, samples were homogenized with 500 μL homogenization buffer (20 mM Tris–HCl, pH 7.4, 10 mM NaCl, 3 mM MgCl$_2$, 0.5% NP-40, 1 mM PMSF, with cocktail protease inhibitor). The homogenate was incubated on ice for 15 min and followed by centrifugation at 3000$g$, 4 °C for 10 min. The nuclear pellet was resuspended in 50 μL nuclear extract buffer (100 mM Tris–HCl, pH 7.4, 100 mM NaCl, 1 mM EDTA, 1% Triton X-100, 0.1% SDS, 10% glycerol, 1 mM PMSF, with cocktail protease inhibitor) and incubated on ice for 30 min with periodic vortexing to resuspend the pellet. After centrifugation, the supernatant for nuclear fractions was collected, boiled in 2× SDS loading buffer for 5 min, and then separated on 10% SDS-polyacrylamide gels. Western blots were performed using antibodies against DNMT3A (1:500, NB120-13888; Novus), H3 (1:1000, 4499; Cell Signaling Technology), GluR1 (1:1000, AB1504; Millipore), GluR2 (1:500, 75-002; NeuroMab), and Actin (1:1000, sc-1616, Santa Cruz).

## Genome-Wide DNA Methylation Analysis

PFC tissue was collected from 4 control and 4 stressed rats (5 days after stress cessation) for genome-wide DNA methylation profiling. Genomic DNA was isolated by using a Zymo DNA isolation kit and quantified by Qubit. The reduced representation bisulfite sequencing (RRBS, Meissner et al. 2005) libraries were prepared by using a Diagenode kit (Cat. No. C02030032). Briefly, 100 ng DNA was digested by MspI, which was then end repaired, adaptor ligated, and size selected by AMPure XP beads. All DNA samples were then treated with sodium bisulfite conversion by using Zymo EZ DNA Methylation-Gold kit. Spike-in control DNAs were included for the monitoring of bisulfite conversion efficiency. The libraries were then purified after PCR amplification. The Agilent bioanalyzer and KAPA library quantification kit were run to ensure the library quality and quantity. A 50-bp single-end sequencing was done on an Illumina HiSeq sequencer with 5% PhiX spike-in.

The quality control for the raw RRBS sequence data was done using FastQC v0.11.7. Trim Galore v0.4.4 (https://www.bioinformatics.babraham.ac.uk/projects/trim_galore/) was then used to perform quality and adapter trimming in 2 subsequent steps. Reads that were determined to be too short (<20 bp) or low quality (Phred Q-score < 20) were filtered. This allows removing of 2 additional bases that contain a cytosine which was introduced in the end-repair step of library preparation. Reanalysis with FastQC was done to confirm the removal of adapter-contaminated and poor quality read segments before moving on to alignment.

RRBS reads were aligned to the rat genome rn6 by bismark v0.19.0 (Krueger and Andrews 2011). To measure the cytosine conversion rate, bsmap v1.0 (Xi and Li 2009) was used to map the Diagenode RRBS unmethylated spike-in to its reference. The resulting BAM files were sorted and indexed using the SAMtools suite (Li et al. 2009), which were then input into the R package methylKit v1.6.1 (Akalin et al. 2012) for differential methylation analysis. Cytosines were filtered to only those that had at least 10 reads of coverage per sample, and remaining cytosines were subsequently normalized. Differentially methylated CpGs were defined as those with SLIM-corrected $P$-value ($q$-value) ≤ 0.05 and an absolute methylation difference ≥15% (Wang et al. 2011).

Annotation of differentially methylated loci was performed by homer_v4.10.4 (Heinz et al. 2010) utilizing the rn6 genome curated by UCSC. We performed pathway analysis based on the differentially methylated CpGs sites using kegga function from the R package Limma v3.36.3 (Ritchie et al. 2015); only differentially methylated CpG loci found in introns, exons, promoter regions (i.e., 1000 bp upstream and 100 bp downstream of TSS), TTS regions (i.e., 100 bp upstream and 1000 bp downstream of TTS), and both 5′ and 3′ untranslated regions (UTRs) were passed to kegga. Key mappings between annotation files were extracted from biomaRt (Durinck et al. 2009) and the Kyoto Encyclopedia of Genes and Genomes using KEGGREST_v1.18.1, a software tool written by Dan Tenenbaum and hosted through the Bioconductor database.

## Sodium Bisulfite Sequencing

Genomic DNA (200 ng) was treated with sodium bisulfite by using the Zymo EZ DNA Methylation-Gold kit following the product protocol. The bisulfite-converted DNA was then used for PCR amplification. The PCR products were purified after running on an electrophoresis gel and cloned for Sanger Sequencing by using the Invitrogen TOPO cloning kit. Minipreps were set up and sequenced. The primer sequences are listed below. *Grid1*: (forward) TTTGTGTTGTTGTTTTTT-GGAGT; (reverse) AAACAAATTAACAAAAACTATTTAAAAA; *Grid2*: (forward) AAAGATTTAG-GTATTTGGGGATTAG; (reverse) ATTCACTACATATAAAAATA-AAAAAAATTC.

## RNA Sequencing

100 ng of total RNA was ribo-depleted using the NEBNext rRNA Depletion Kit (New England Biolabs, Inc., Ipswitch, MA) following the manufacturer's protocol. Ribo-depleted RNA sequencing (RNAseq) libraries were constructed through the NEBNext Ultra II Directional RNA Library Prep Kit for Illumina (New England Biolabs, Inc., Ipswich, MA). RNA samples were fragmented, and cDNA was synthesized from the first and second strands, consecutively. The ends of cDNA fragments were ligated with universal Illumina adapters. RNAseq libraries were individually indexed with NEBNext Multiplex Oligos for Illumina

(New England Biolabs, Inc., Ipswich, MA) and amplified through 11 cycles of PCR amplification. All clean-up steps were accomplished by using the supplied purification beads within the NEBNext Ultra II Directional RNA Library Prep Kit.

RNA-seq reads were assessed for quality control using FastQC v0.11.8 (https://www.bioinformatics.babraham.ac.uk/projects/fastqc/) with Illumina adapter sequences, low-quality bases, and sequencing artifacts using Trimmomatic v0.36 (Bolger et al. 2014). Trimmed reads were aligned to the rn6 reference genome using hisat2 v2.1.0 (Kim et al. 2019) with default parameters. Successfully mapped read alignments were then assigned to gene features in the rn6 reference gene annotation file using featureCounts v1.5.0-p3 (Liao et al. 2014) ignoring multi-mapping and multi-overlapping read alignments. Raw gene counts were normalized using the TMM: trimmed mean of M-values method (Robinson and Oshlack 2010), and genes with greater than 0.5 counts per million in at least 4 or more samples were assessed for differential gene expression using EdgeR v3.20.9 (Robinson and Oshlack 2010). To assess the biological significance of differentially expressed genes, we tested genes passing FDR < 0.05 filters with an overrepresentation test of KEGG curated pathways (Kanehisa et al. 2019), once again using the Limma v3.36.3 (Ritchie et al. 2015) implementation of kegga.

## Visualization of Sequencing Data

To represent the association between differentially methylated CpGs and the differentially expressed genes, CpGs that were annotated in the gene body of differentially expressed genes, which include TSS, exon, intron, TTS, and both UTRs, were connected with corresponding gene expression data. The direction of effects, in both log2FC and methylation difference, was binarized to either −1 or 1 representing negative effect change or positive effect change, respectively. Next, each binarized effect direction was multiplied by the significance of the respective calculation and plotted on the axes, where x-axis represents differential methylation and the y-axis represents differential gene expression. To represent the interaction of differentially methylated CpGs in promoter regions of differentially expressed genes, we connected corresponding gene expression data to these CpGs and plotted them in the same manner as above, with binarized effect changes multiplied by the corresponding significance values. The plots were created using the Bioconductor package ggplot2.

## Statistics

Experiments with 2 groups were analyzed statistically using unpaired Student's t-tests with unequal variance. Experiments with more than 2 groups were subjected to one-way or two-way analysis of variance (ANOVA), followed by Bonferroni post hoc tests. The value of $P < 0.05$ was considered as being significantly different among groups.

## Results

### DNA methyltransferase *Dnmt3a* Is Downregulated in the PFC of Animals Exposed to Chronic Unpredictable Stress

As chronic unpredictable stress often has profound effects that outlast the stress duration, we speculate that DNA methylation, which provides lasting changes in chromatin remodeling and gene transcription, is potentially involved in the sustained action of stress. To test this, we examined DNA methyltransferases (*Dnmts*) in PFC of rats exposed to 2-week unpredictable stress at 7 days after stress cessation. Quantitative RT-PCR analyses indicated that the mRNA level of *Dnmt3a* and *Dnmt3b*, but not *Dnmt1*, was significantly lower in PFC lysates from stressed animals (Fig. 1A, n = 11 pairs, *Dnmt3a*: $0.60 \pm 0.10$ fold of control, $t_{(19)} = 2.98$, $P < 0.01$; *Dnmt3b*: $0.58 \pm 0.10$ fold of control, $t_{(19)} = 2.97$, $P < 0.01$; *Dnmt1*: $0.95 \pm 0.09$ fold of control, $t_{(18)} = 0.43$, $P > 0.05$, t-test). In addition, we also measured the expression of ten-eleven translocation (*Tet*) enzymes, which play an important role in DNA demethylation by oxidizing 5mC (Tahiliani et al. 2009). The mRNA levels of the 3 members of *Tet* family, *Tet1*, *Tet2*, and *Tet3*, were not significantly changed in stressed animals (Fig. 1B, n = 4 pairs, *Tet1*: $0.85 \pm 0.03$ fold of control, $t_{(3)} = 1.62$, $P > 0.05$; *Tet2*: $1.07 \pm 0.07$ fold of control, $t_{(4)} = -0.31$, $P > 0.05$; *Tet3*: $1.02 \pm 0.04$ fold of control, $t_{(4)} = -0.072$, $P > 0.05$, t-test). Since a substantial amount of DNMT3A was detected in postmitotic CNS neurons (Feng et al. 2005), western blotting was performed to compare the protein level of DNMT3A in the nucleus fraction of PFC tissue from rats with or without stress exposure. As shown in Figure 1C, stressed animals showed significantly decreased protein level of DNMT3A (n = 4 pairs, $35.3\% \pm 9.9\%$ decrease, $t_{(4)} = 3.54$, $P < 0.05$, t-test). These data demonstrated that chronic unpredictable stress induces the suppression of DNMT3A, which suggest a potential DNA methylation change at its target genes.

### The Effect of Chronic Unpredictable Stress on AMPAR Expression and Function in PFC Was Reproduced by DNMT Inhibitors

To find out the consequence induced by chronic unpredictable stress, we examined the expression and functions of glutamate receptors that mediate excitatory transmission in the central nervous system. Quantitative RT-PCR and western blotting were performed to examine the mRNA and protein levels of AMPAR subunits in PFC from rats exposed to 2-week unpredictable stress at 7 days after stress cessation. As shown in Figure 2A, stressed animals had a significantly decreased mRNA level of AMPAR subunit *Gria2*, but not *Gria1* (*Gria2*: $0.51 \pm 0.11$ fold of control, n = 5 pairs, $t_{(7)} = 2.56$, $P < 0.05$, t-test; *Gria1*: $0.87 \pm 0.11$ fold of control, n = 6 pairs, $t_{(9)} = 0.83$, $P > 0.05$, t-test). Consistently, the corresponding protein level of AMPAR subunit GluR2, but not GluR1, was significantly decreased in stressed animals (Fig. 2B, GluR2: $30.8\% \pm 5.7\%$ decrease, n = 9 pairs, $t_{(13)} = 4.55$, $P < 0.01$, t-test).

To test whether the altered AMPAR expression is related to DNMT, we injected a DNMT inhibitor, RG108, into the PFC of unstressed control rats and examined the level of AMPAR subunits. Compared to vehicle-injected rats, RG108-injected rats exhibited a significant reduction of GluR2, but not GluR1 (Fig. 2B, n = 8 pairs, GluR1: $-3\%$ decrease, $t_{(9)} = -0.24$, $P > 0.05$, t-test; GluR2: $34\%$ decrease, $t_{(9)} = 3.52$, $P < 0.01$, t-test), which is reminiscent to the effect of chronic unpredictable stress.

The downregulated GluR2 by chronic unpredictable stress or DNMT inhibitors could result in the impairment of glutamatergic transmission in PFC. To test this, we examined the input/output curves of AMPAR-mediated EPSC induced by a series of stimulus intensities in PFC pyramidal neurons. As shown in Figure 2C, AMPAR-EPSC was markedly reduced in PFC neurons of stressed animals (53–60% decrease, $P < 0.05$, two-way ANOVA, n = 16–17 per group). Similarly, AMPAR-EPSC was also significantly decreased in unstressed control rats (p21–23) injected with the DNMT inhibitor 5AzaC (Fig. 2D, 5 mg/kg, i.p., once
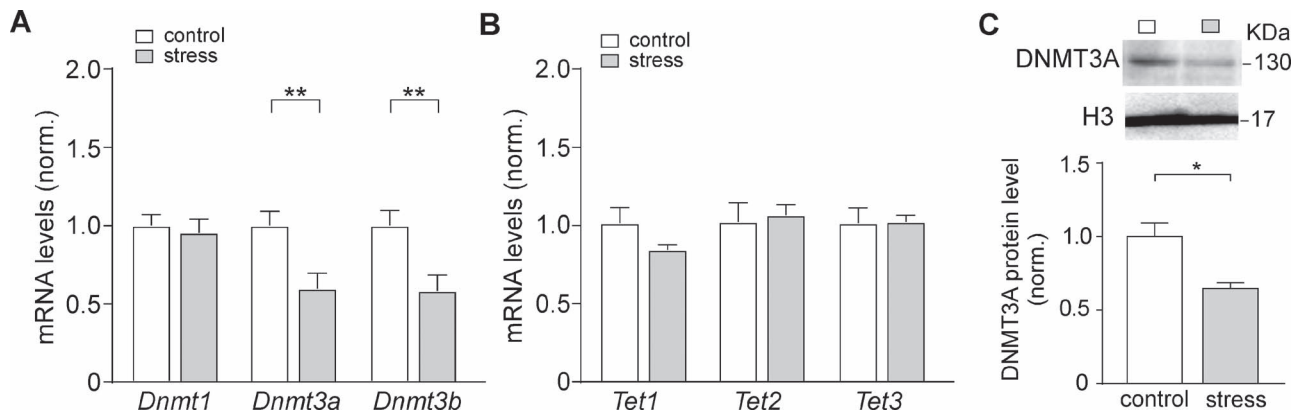
**Figure 1.** *Dnmt3a* is downregulated in PFC of stressed animals. (A, B) Quantitative real-time RT-PCR data on the mRNA level of *DNMT* family members (A) and *TET* family members (B) in PFC from control groups versus stressed rats (exposed to 14-day chronic unpredictable stress). Tests were conducted at 7 days after stress cessation. **$P < 0.01$, t-test. (C) Immunoblots and quantification analysis of the protein level of DNMT3A and Histone H3 in the nuclear fraction of PFC pyramidal neurons from control (con) versus stressed rats. *$P < 0.05$, t-test.

daily for 4–5 days, 41–50% decrease, $P < 0.05$, two-way ANOVA, $n = 11$–12 per group) or RG108 (Fig. 2E, 100 μM, stereotaxic into PFC, 2 μL, 45–51% decrease, $P < 0.05$, two-way ANOVA, $n = 13$–14 per group). In contrast, the $GABA_A$R-IPSC in control rats was not significantly changed by administration of 5AzaC (Fig. 2F, $P > 0.05$, two-way ANOVA, $n = 5$–6 per group) or RG108 (Fig. 2G, $P > 0.05$, two-way ANOVA, $n = 10$–11 per group). Taken together, these results suggest that chronic unpredictable stress induces the sustained loss of GluR2 expression and AMPAR function in PFC, and this effect can be mimicked by DNMT inhibition in unstressed control animals.

### Overexpression of *Dnmt3a* in the PFC Rescues Stress-Induced AMPAR Dysfunction

To further test the involvement of DNMTs in the synaptic transmission of chronic unpredictable stress, we used the herpes simplex virus (HSV)-mediated gene transfer (Fink et al. 1996) to overexpress *Dnmt3a* (LaPlant et al. 2010) in stressed animals. The *GFP*-HSV or *Dnmt3a*-HSV (GFP-tagged) was bilaterally injected into prelimbic regions on the next day after stress cessation (Fig. 3A), and recordings were performed 3 days after viral injection. As shown in Figure 3B, stressed animals injected with the GFP control HSV (stress+GFP) had the significantly reduced AMPAR-EPSC (47–57% decrease, $n = 10$–13 per group, $F_{3,44 \text{(group)}} = 9.3$, $P < 0.001$, two-way repeated-measure ANOVA), and *Dnmt3a*-HSV injection to stressed animals (stress+DNMT3A) restored AMPAR-EPSC to the control level ($n = 13$, $P > 0.05$, compared to con+GFP). *Dnmt3a*-HSV injection to the control group (con+DNMT3A) did not significantly alter the amplitude of AMPAR-EPSC ($n = 12$, $P > 0.05$, compared to con+GFP). Together, these electrophysiological results suggest that DNMT3A is a key factor required for the downregulation of AMPAR responses by chronic unpredictable stress.

### DNMT3A Contributes to Behavioral Alterations in Animals Exposed to Chronic Unpredictable Stress

To determine the role of DNMT in behavioral alterations induced by chronic unpredictable stress, we examined TOR memory, a cognitive process mediated by PFC (Barker et al. 2007; Yuen et al. 2012), in rats exposed to 2-week unpredictable stress at 7 days after stress cessation. As shown

in Figure 4A, control animals (con+GFP) spent significantly more time exploring the novel (less recent) object than the familiar object (novel object: $17.2 \pm 2.5$ s, familiar object: $7.4 \pm 1.5$ s, $n = 6$, $t_{(8)} = 3.38$, $P < 0.01$, t-test). The preference of the novel object was lost in stressed rats (stress+GFP, novel object: $15.4 \pm 2.7$ s, familiar object: $14.7 \pm 3.0$ s, $n = 6$, $t_{(9)} = 0.18$, $P > 0.05$, t-test) but was restored by overexpression of DNMT3A in stressed rats (stress+DNMT3A, novel object: $13.1 \pm 1.4$ s, familiar object: $5.3 \pm 0.9$ s, $n = 6$, $t_{(8)} = 4.64$, $P < 0.01$, t-test). The DR, an index of the object recognition memory, indicated the profound impairment of TOR memory by chronic unpredictable stress, which was rescued after *Dnmt3a*-HSV injection into the PFC (Fig. 4B, con+GFP: $42.2\% \pm 7.5\%$, $n = 6$; stress+GFP: $4.3\% \pm 2.7\%$, $n = 6$; stress+DNMT3A: $42.8\% \pm 6.9\%$, $n = 6$; con+DNMT3A: $58.4\% \pm 6.9\%$, $n = 6$; $F_{1,20 \text{(animal)}} = 17.9$, $P < 0.001$, $F_{1,20 \text{(treatment)}} = 18.8$, $P < 0.01$, two-way ANOVA). The total exploration time on both objects in sample phases I and II had no significant difference between groups, while the groups injected with *Dnmt3a*-HSV show slightly lower exploration time in the test phase, compared with GFP-injected groups ($F_{1,20 \text{(animal)}} = 6.61$, $P < 0.05$, $F_{1,20 \text{(treatment)}} = 0.71$, $P > 0.05$, two-way ANOVA).

In addition to TOR memory task, we measured aggression-like behaviors in RI tests. Rats exposed to chronic unpredictable stress exhibited significantly increased attack durations, while the effect was partially attenuated in the stressed animals with PFC injection of *Dnmt3a*-HSV in RI tests (Fig. 4C, control+GFP: $34.8 \pm 9.6$ s, $n = 8$; stress+GFP: $106.2 \pm 15.6$ s, $n = 8$; stress+DNMT3A: $73.8 \pm 11.6$ s, $n = 11$; control+DNMT3A: $51.0 \pm 11.8$ s, $n = 6$; $F_{1,29 \text{(animal)}} = 12.3$, $P < 0.01$, $F_{1,29 \text{(interaction)}} = 4.2$, $P < 0.05$, two-way ANOVA).

Locomotive activity of the 4 groups was also measured. As shown in Figure 4D, rats exposed to chronic unpredictable stress had higher locomotive activity than controls, which was partially reduced by DNMT3A overexpression at PFC (# midline crossing, con+GFP: $16.0 \pm 1.65$, $n = 7$; stress+GFP: $24.3 \pm 2.58$, $n = 7$; stress+DNMT3A: $19.3 \pm 0.62$, $n = 9$; con+DNMT3A: $19.8 \pm 1.45$, $n = 6$; $F_{1,23 \text{(animal)}} = 0.17$, $P > 0.05$, $F_{1,23 \text{(treatment)}} = 4.51$, $P < 0.05$, two-way ANOVA).

Furthermore, we performed a variety of anxiety- and depression-related behavioral tests, including open-field, elevated plus maze, light–dark box, novelty-suppressed feeding, social approach, and sucrose preference, but no significant difference was found between control ($n = 10$) versus stressed
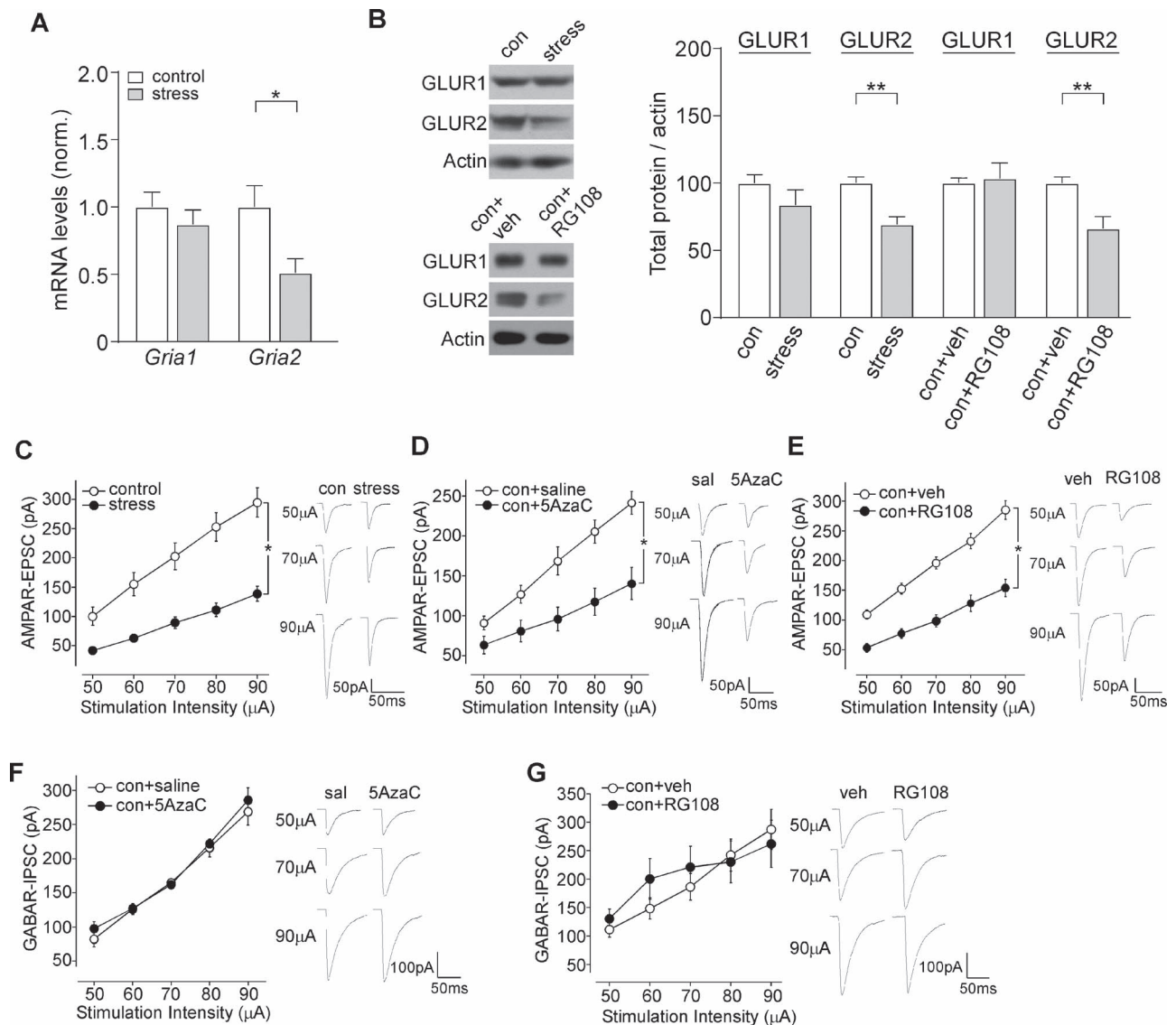
**Figure 2.** DNMT inhibitors reproduce the effect of chronic unpredictable stress on AMPAR expression and function in PFC. (A) Quantitative real-time RT-PCR data on the mRNA level of AMPAR subunits *Gria1* and *Gria2* in PFC from control versus stressed animals. *P < 0.05, t-test. (B) Immunoblots and quantification analysis of AMPAR subunits in PFC from control (con) versus stressed rats or control rats with the PFC injection of RG108 versus vehicle. **P < 0.01, t-test. (C–E) Summarized input–output curves of AMPAR-EPSC in PFC neurons from control versus stressed rats (C), or control rats i.p. injected with 5AzaC versus saline (D), or control rats with the PFC injection of RG108 versus vehicle (E). *P < 0.05, two-way ANOVA. Inset: representative EPSC traces. (F, G) Summarized input–output curves of GABA_AR-IPSC in PFC neurons from control rats i.p. injected with 5AzaC versus saline (F), or control rats with the PFC injection of RG108 versus vehicle (G). Inset: Representative IPSC traces.

($n = 10$) groups (Fig. 4E–J). Taken together, these results suggest that DNMT3A plays an important role in regulating some stress-induced behavioral changes, including recognition memory deficits, elevated aggression, and hyperlocomotion.

## Genome-Wide DNA Methylation Changes and Transcriptome Alterations in PFC of Stressed Rats

Given the alteration of DNMT3 expression in the PFC of stressed animals, we hypothesized that this is accompanied with DNA methylation changes across genome. To test this, we performed genome-wide DNA methylation profiling. We carried out RRBS (Meissner et al. 2005) on 4 pairs of animals. The sequencing data are of good quality (Supplementary Table 1). The average mapping efficiency is 67.9% and the bisulfite conversation rate for each library is over 99%.

We then performed differential analysis and identified 11 558 hypomethylated CpG sites and 13 800 hypermethylated CpGs (Supplementary Table 2), suggesting that DNA methylome homeostasis is affected by stress. The role of DNA methylation on gene transcription is better studied at gene promoters, where methylation normally represses gene transcription. Although RRBS has a preferred coverage on gene promoters (19.9%, Fig. 5A), we observed fewer differential DNA methylation sites in this area (6.0% of all differential sites, Fig. 5B). Instead, the majority of differential DNA methylation sites is located in intergenic regions and introns (56.3% and 27.2% of total differential sites, respectively, Fig. 5B). Moreover, a small but consistent portion of differential sites exists in exons and transcription termination sites (TTS). This indicates that DNA methylation changes in stressed brain may have broader effects across thegenome.
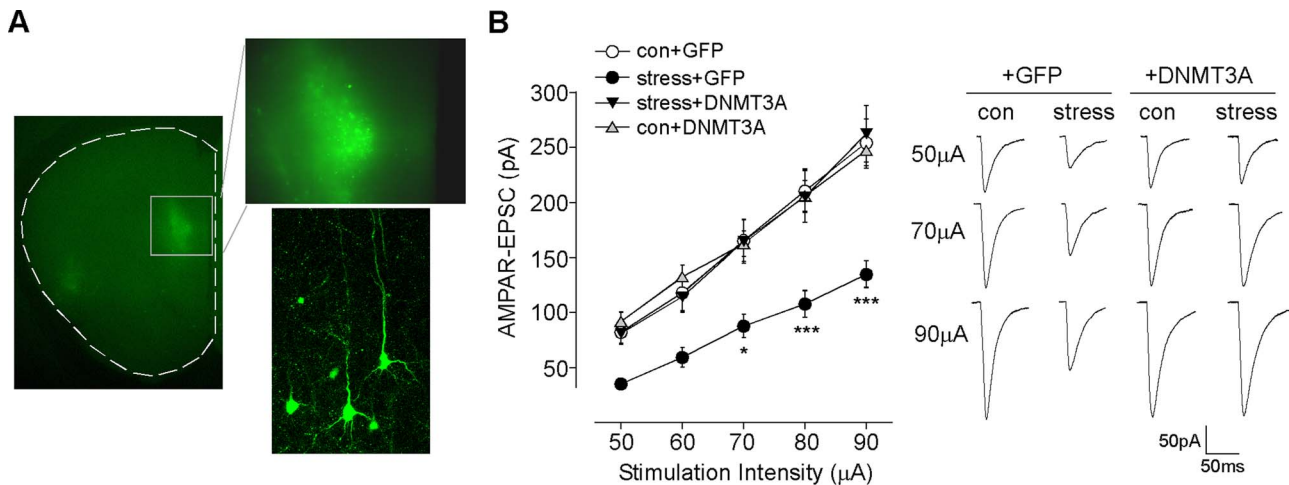
**Figure 3.** Expression of DNMT3a in the PFC of stressed animals rescues AMPAR function. (*A*) Left, A low-magnification image of a coronal slice showing the *Dnmt3a*-HSV-infected medial PFC region. Right, A confocal image of DNMT3a-HSV-infected PFC neurons. (*B*) Summarized input/output curves of AMPAR-EPSC in control (con) versus stressed rats with the PFC injection of *Dnmt3a*-HSV or *GFP*-HSV. *$P < 0.05$, ***$P < 0.001$, two-way ANOVA. Inset: Representative AMPAR-EPSC traces.

To gain insights into the potential function of these DNA methylation changes, we examined the gene ontology pathways enriched with differentially methylated sites. Given the difficulty to link DNA methylation changes at intergenic regions to their target genes, we limited this analysis to the gene proximal regions that include promoter, exon, intron, TTS, and UTRs. We therefore found numerous pathways that are enriched with methylation changes (Supplementary Table 3), which is indicative of the molecular underpinnings of stress. Among them, axon guidance is one of the top-ranked pathways, which may modulate synaptic connectivity and neural plasticity. Additionally, Wnt and *β*-catenin signaling pathway, which has been shown to regulate stress susceptibility (Wilkinson et al. 2011; Dias et al. 2014), also ranks high in the Gene Ontology (GO) analysis. We also found that DNA methylation changes are highly enriched in several neurotransmitter pathways, such as GABAergic synapse, glutamatergic synapse, and cholinergic synapse, which is consistent with the aberrant synaptic transmission we recognized via electrophysiology assays (Figs 2 and 3). Neurotrophic factors, such as BDNF, are believed to play critical roles in synaptic response to stress. Concomitantly, we further found that BDNF downstream signaling cascades, such as microtubule-associated protein kinase (MAPK) and Rap1 (Ras-related protein 1) signaling pathways, are enriched with DNA methylation changes. Taken together, we found that genome-wide DNA methylation changes in stressed brains are selectively clustered in pathways that play important roles in synaptic plasticity and neural signaling.

To gain more insight of the gene transcription regulation that is associated with the observed DNA methylation changes, we then performed RNA-seq experiments (Supplementary Table 4) to assess differential gene expression in rat PFC after chronic stress. We found numerous differentially expressed genes (Supplementary Table 5) with most of them are upregulated. We then identified the differential genes that have DNA methylation changes at either gene promoters (Supplementary Table 6) or gene bodies (Supplementary Table 7). We found that both hypermethylation and hypomethylation changes can exist at genes that have transcription increase or decrease, which suggests a complex interaction between DNA methylation and transcription (Fig. 5C,D). To assess the biological significance

of the differentially expressed genes, we calculated their overrepresented KEGG curated pathways (Supplementary Table 8). Interestingly, we found that most differentially expressed genes' enriched pathways are also enriched with differential methylation changes, which include glutamatergic synapse, MAPK signaling, hippocampal signaling, PI3K-Akt signaling pathway, etc. (Fig. 5E). This suggests that the stress-induced transcription changes mainly occur in the gene networks that have the accompanying DNA methylation alterations, which indicates an important role of DNA methylation in transcription regulation during stress development.

Among the genes that demonstrate both methylation and transcription alterations after stress, we found a decrease of DNA methylation at the gene body of *Grid1* and *Grid2*, which is associated with their mRNA increase. *Grid1* and *Grid2* encode *δ*1 and *δ*2 glutamate receptors (GluD1, GluD2), receptively. GluD2 has been implicated in regulating the endocytosis of AMPA receptor GluR2 and GluR2-mediated neural plasticity (Kohda et al. 2013a, 2013b). We then carried out sodium bisulfite sequencing to target the genomic region that includes the differential methylation sites (Fig. 6A,B). For the 7 CpG sites located within the approximately 250-bp intronic region of *Grid1*, there is a general decrease of DNA methylation, especially at the first 2 CpG sites at the 5′ of this locus. Within the approximately 310-bp intronic region of *Grid2*, there is a small but consistent decrease of DNA methylation across the first 3 CpG sites that are included in this region. Quantitative PCR confirmed the stress-induced transcriptional increase of *Grid1* and *Grid2* genes (Fig. 6C, control: $n = 7$, stress: $n = 6$, *Grid1*: $t_{(9)} = 4.0$, $P < 0.01$; *Grid2*: $t_{(8)} = 3.3$, $P < 0.05$, *t*-test). Additionally, by using qPCR, we confirmed the RNAseq-detected mRNA increase of transcription regulators, *Hdac7* and *Zfp423* (Fig. 6C, control: $n = 7$, stress: $n = 6$, HDAC7: $t_{(5)} = 3.0$, $P < 0.05$; Zfp423: $t_{(5)} = 4.6$, $P < 0.01$, *t*-test), which may contribute to the alterations of target genes in our stress model.

## Discussion

Epigenetic mechanisms, such as DNA methylation, play an important role in regulating gene expression, which underlies
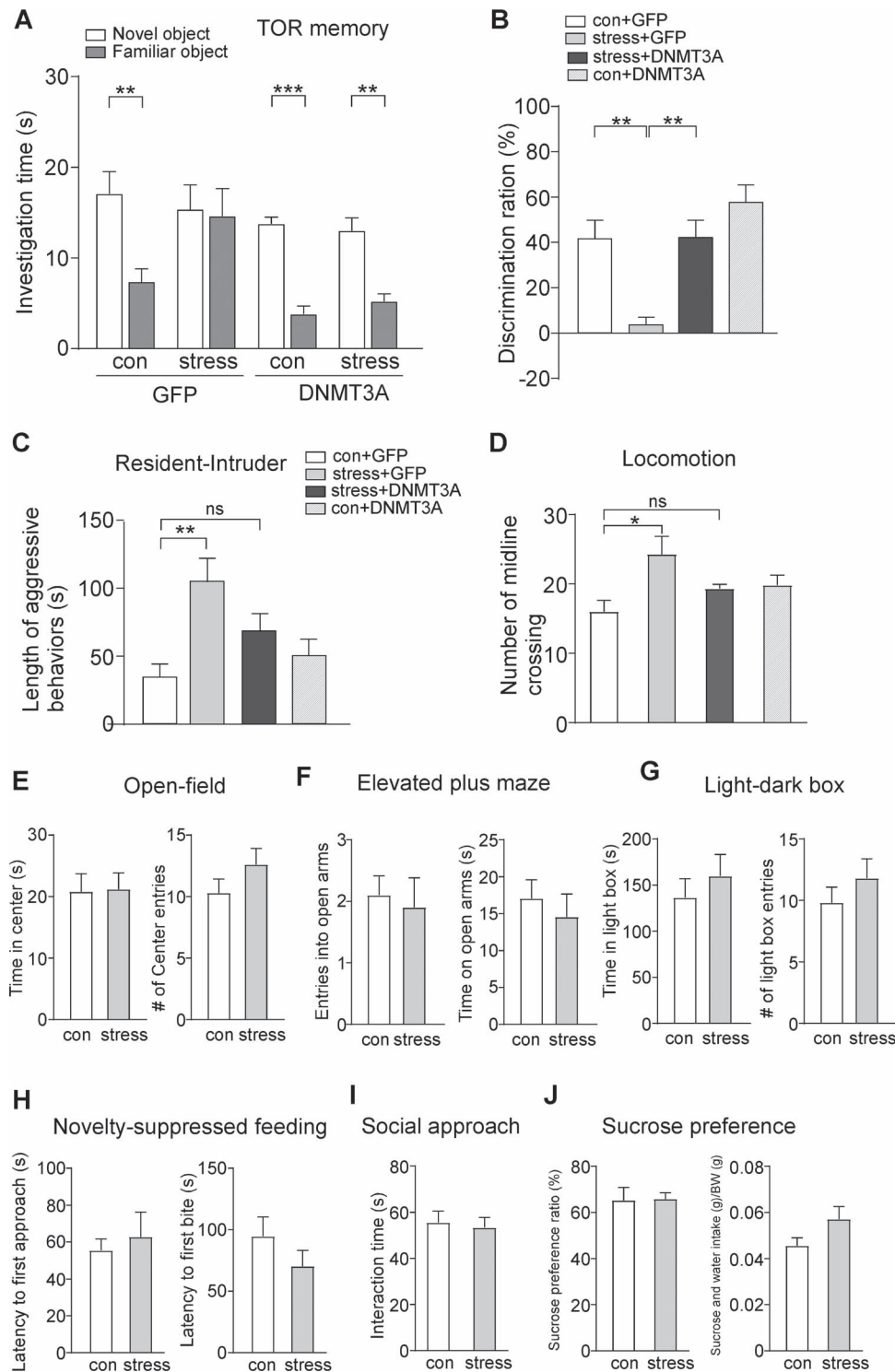
**Figure 4.** Expression of DNMT3a in the PFC of stressed animals attenuates some behavioral deficits. (*A*, *B*) Bar graph (mean ± SEM) showing the exploration time of novel versus familiar objects (*A*) and DR (*B*) of TOR memory task in control versus stressed rats with the PFC injection of *Dnmt3a*-HSV or *GFP*-HSV. **$P < 0.01$, ***$P < 0.001$, *t*-test (*A*) or two-way ANOVA (*B*). (*C*) Bar graphs showing the duration of attacks in the RI test of control versus stressed animals injected with *Dnmt3a*-HSV or *GFP*-HSV. **$P < 0.01$, two-way ANOVA. (*D*) Bar graphs showing the number of midline crossing in the locomotion test of control versus stressed rats with the PFC injection of *Dnmt3a*-HSV or *GFP*-HSV. *$P < 0.05$, two-way ANOVA. (*E*) Bar graphs showing the time spent at the center and the number of center entries in the open-field test of control versus stressed rats. (*F*) Bar graphs showing the number of open arm entries and the time spent in open arms in the elevated plus maze test of control versus stressed rats. (*G*) Bar graphs showing the time spent in the light chamber and the number of light chamber entries in the light–dark box test of control versus stressed rats. (*H*) Bar graphs showing the latencies of first approaching and first consuming of a food pellet in the novelty-suppressed feeding test of control versus stressed rats. (*I*) Bar graphs showing the total time of interaction with the social stimulus in the social approach test of control versus stressed rats. (*J*) Bar graphs showing the sucrose preference ratio and the total volume consumption in the sucrose preference test of control versus stressed rats.
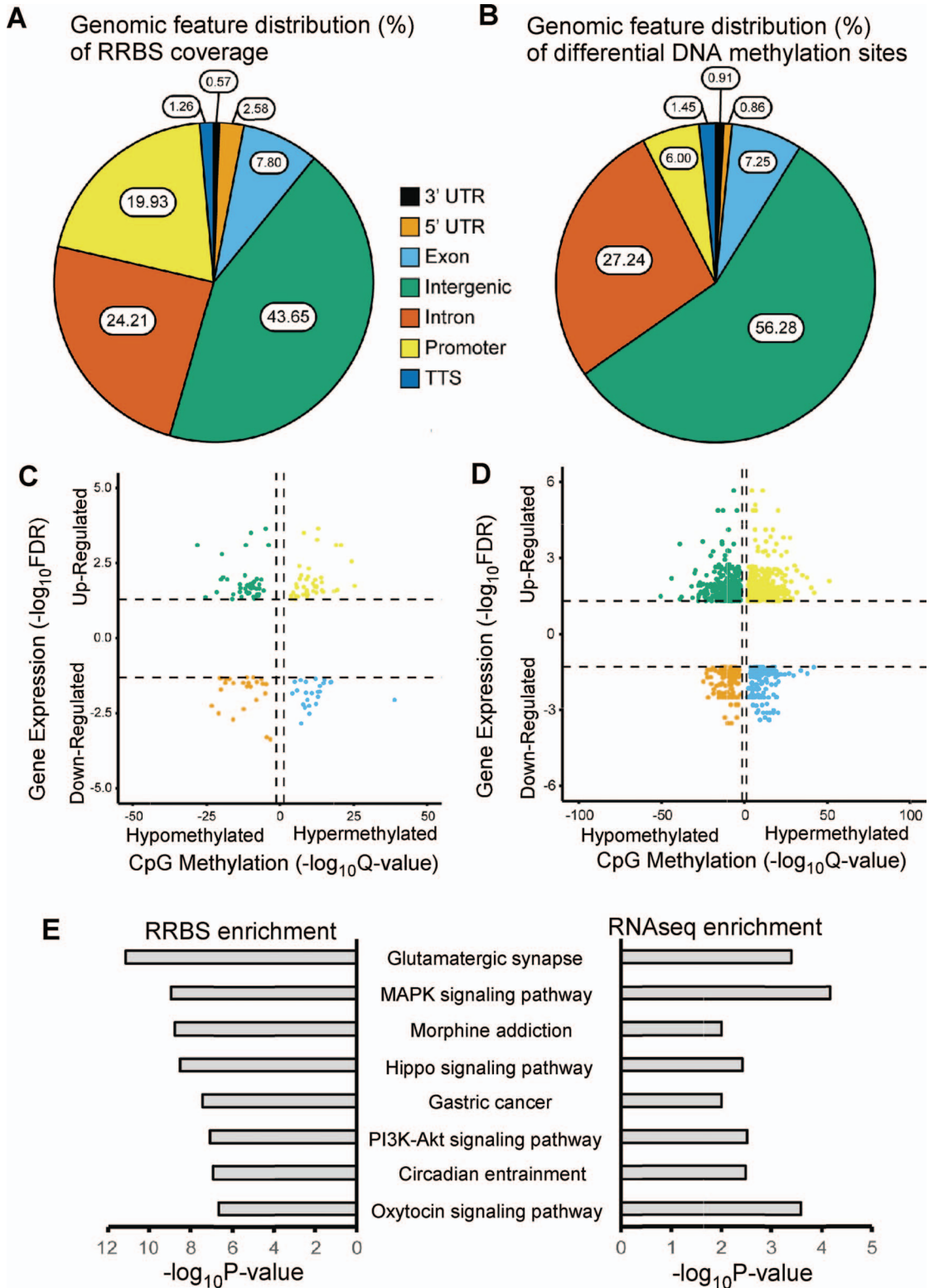
**Figure 5.** Genome-wide DNA methylation changes and transcription alterations in PFC of stressed animals. (A, B) Genomic feature distributions (%) of total DNA coverage sites (A) or differential DNA methylation sites (B). (C, D) Scatter plots representing differential methylation loci (DML) within annotated gene promoters (C) or gene loci (D) and their corresponding differentially expressed genes. Gene loci were defined as a region from TSS to TTS, including 5′ UTR, intron, exon, and 3′ UTRs. The x-axis represents significance of differentially methylated loci with either increased (hypermethylated) or decreased (hypomethylated) DNA methylation change. The y-axis represents the significance of differential gene expression. Vertical and horizontal dashed lines represent significantly changed CpG methylation and gene expression, respectively. (E) Top overlapping KEGG pathways that are significantly overrepresented in differentially methylated CpGs (RRBS) and differentially expressed genes (RNAseq). Differentially methylated CpGs were characterized as within genic loci if they were found in promoter regions, 5′ and 3′ UTRs, introns, exons, and TTS regions.
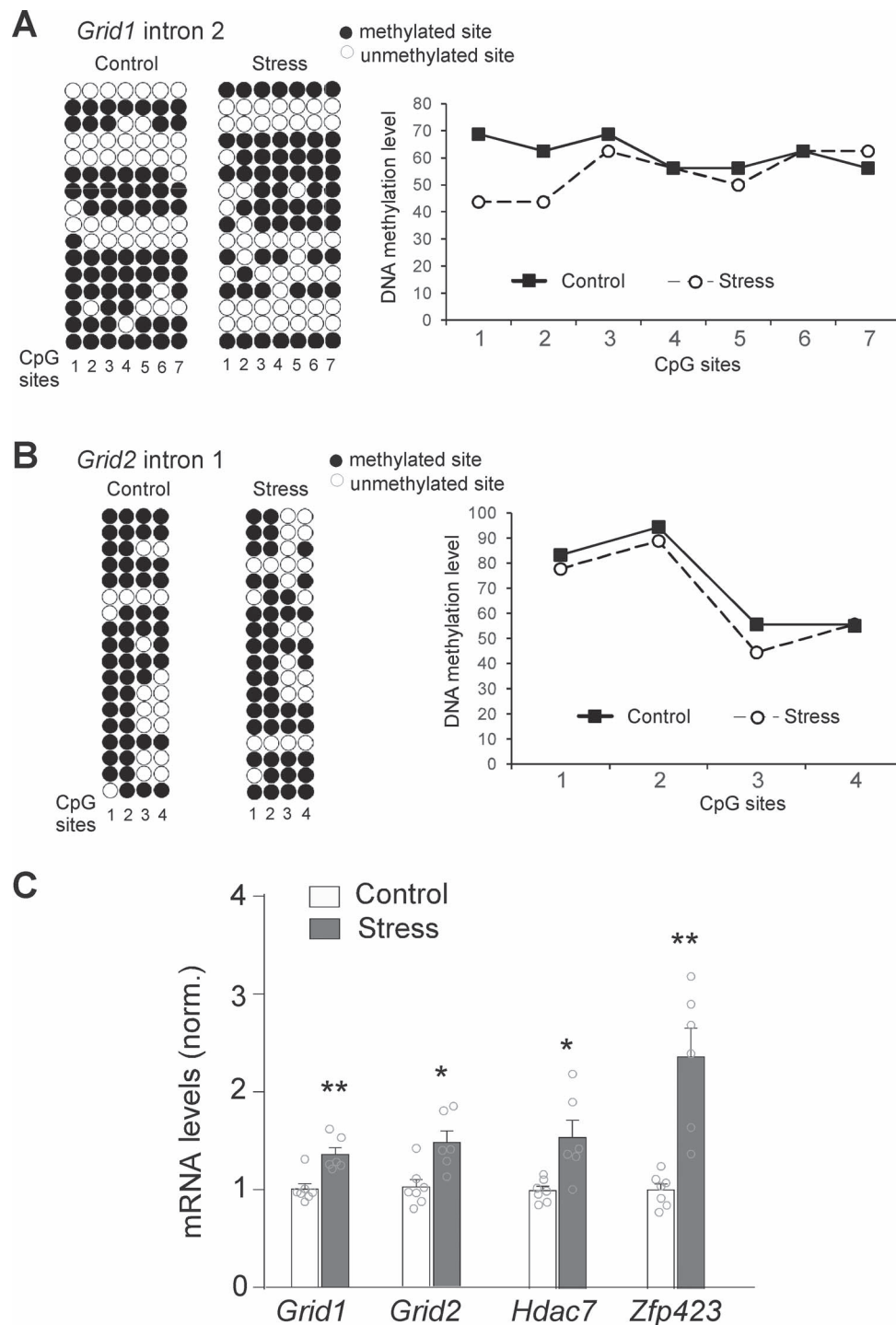
**Figure 6.** Validation of DNA methylation and gene transcription changes. (*A*, *B*) Sodium bisulfite sequencing analysis of *Grid1* and *Grid2* gene DNA methylation status in rat PFC after chronic unpredictable stress. The analysis covers 7 CpG sites in intron 2 region of *Grid1* gene (Chr16: 11 198 532–11 198 784) and 4 CpG sites in intron 1 region of *Grid2* gene (Chr4: 94 103 991–94 104 301). On the left, each row represents DNA methylation data derived from 1 clone (black dots: methylated sites, white dots: unmethylated sites). The average methylation levels at these CpG sites are shown in the line graph on the right. *Grid1* CpG sites 3 and 4, as well as *Grid2* CpG site 3, were detected by RRBS differential analysis (Supplementary Table 7). (*C*) Quantitative RT-PCR analysis on the mRNA levels of *Grid1*, *Grid2*, *Hdac7*, and *Zfp423* in rat PFC after chronic unpredictable stress. Their transcription increases were also recognized by RNAseq (Supplementary Table 5). *$P < 0.05$, **$P < 0.01$, *t*-test.

basic brain function and behavior (Day and Sweatt 2011; Shin et al. 2014). Accumulating evidence implicated DNA methylation's role in synaptic transmission, plasticity, learning, and memory (Levenson et al. 2006; Dulac 2010; Yu et al. 2011; Morris and Monteggia 2014; Muñoz et al. 2016). For example, in vitro studies demonstrated that the treatment of hippocampal

cultures with methylcytosine analog 5AzaC decreases the frequency of miniature EPSCs without altering the excitatory synapse numbers (Nelson et al. 2008). Hippocampal plasticity and function were found to be impaired in *Dnmt1* and *Dnmt3a* double knockout mice (Feng et al. 2010). Persistent gene-specific cortical hypermethylation was induced by a single hippocampus-dependent associative learning experience, and pharmacological inhibition of DNA methylation disrupts the remote memory (Miller et al. 2010).

The relative stability of covalent coupling of methyl group to DNA base may also serve as a lasting epigenetic modification associated with the sustained aberrant behavior, such as those occur in stress response. For example, early-life maternal adversity alters DNA methylation status of offspring's GR gene, leading to persistent GR expression changes and hypothalamic–pituitary–adrenal responses to stress in adulthood (Turecki and Meaney 2016). Moreover, a foot-shock stress was found to affect the expression of DNMT as well as DNA methylation in rat hippocampus (Miller and Sweatt 2007). Chronic social defeat stress also decreases the global DNA methylation level in mouse medial PFC, and *Dnmt3a* overexpression in the medial prefrontal cortex (mPFC) of stressed mice attenuates stress-induced anxiety (Elliott et al. 2016). Furthermore, TET1, the enzyme regulating DNA demethylation, was also implicated in depression- and anxiety-like behaviors in mouse nucleus accumbens (Feng et al. 2017), further elucidating the role of DNA methylation dynamics in depression.

In this study, we revealed that altered DNMT3A is also implicated in the sustained synaptic and behavioral deficits induced by chronic unpredictable stress. Inhibiting DNMT activity in control animals recapitulates the stress-induced impairment of *Gria2* expression, glutamatergic transmission, and PFC-dependent recognition memory, while overexpression of *Dnmt3a* in PFC of stressed animals prevents AMPAR hypofunction and behavioral deficits. These results therefore suggest the important role of DNA methylation in some effects of chronic unpredictable stress.

Here, we have focused the electrophysiological recordings on prelimbic pyramidal neurons, because prelimbic cortex is one of the key PFC regions mediating the synaptic and behavioral effects of repeated stress (Radley et al. 2005, 2006, 2008; Yuen et al. 2012; Maeng and Shors 2013). Other PFC regions (e.g., infralimbic cortex, anterior cingulate cortex) are also important components in the stress networks (Wilber et al. 2011; Yoshida et al. 2018; Piggott et al. 2019; Ito et al. 2020), and it awaits to be tested whether they exhibit similar changes.

Although we have detected the stress-induced decrease of *Dnmt3a* and *Gria2* expression with qPCR, these genes were not identified in RNAseq differential analyses with various combinations of alignment, gene feature assignment, and normalization pipelines. It is known that RNAseq from different cohorts of samples tends to discover differential gene sets that do not fully overlap. Moreover, RNAseq data do not always agree with qRT-PCR results, which may be due to the different intrinsic sensitivity and positive/negative discovery rates of each methodology. The samples used in qPCR and RNAseq in this study were from different cohorts of animals that may carry biological variations. Our qPCR data were derived from 11 pairs of animals with big individual variations within the group. We suspect that the limited sample size in RNAseq ($n = 4$/group) may limit our ability to capture the expression changes in *Dnmt3a* and *Gria2*.

Concomitant with the alteration of DNMT expression in PFC after chronic unpredictable stress, we found numerous hyper- and hypomethylation sites across the genome. This is consistent with the previous observations that both directions of epigenetic alterations usually occur across the genome when the corresponding catalyzing enzyme is altered. Furthermore, when we overlay the genes that demonstrate both methylation and transcription changes, we found that the transcription increase or decrease can be associated with either DNA hypermethylation or hypomethylation (i.e., hypermethylation vs. transcription decrease, hypermethylation vs. transcription increase, hypomethylation vs. transcription decrease, hypomethylation vs. transcription increase). Considering the diverse cellular heterogeneity in the brain, DNMT and DNA methylation may only change in a specific cell type (Lister et al. 2013). To better elucidate the interaction between DNA methylation and transcription in stress, it will be important to profile DNA methylome and transcriptome in a cell type-specific manner in the future. This may reveal the methylation change in *Gria2* gene after stress, as the change in a defined cell type could be masked by the current heterogeneous tissue-based profiling.

It is also possible that *Gria2* is not a direct target of DNMT3A. Given the general silencing role in gene expression by DNA methylation, we speculate that the stress-associated DNMT3A reduction may induce the disinhibition and upregulation of some negative regulators of *Gria2*. We have confirmed the RNAseq results on the transcriptional induction of *Hdac7* and *Zfp423* through qPCR. As both can serve as transcription regulators, particularly HDAC7 is known to repress gene transcription, it will be important to evaluate their interaction with *Dnmt3a* and *Gria2* genes in the future. Nevertheless, we should emphasize that the convergent pathways enriched in differential DNA methylation and gene transcription are selectively clustered in several neural function-related categories, such as glutamate receptor signaling. This coexistence reveals that stress-induced transcription changes mainly occur in the gene networks that have the accompanying DNA methylation alterations, further suggesting a role of DNA methylation in stress effects. Interestingly, consistent with what we found in RRBS and RNAseq, we have detected the DNA methylation decrease at *Grid1* and *Grid2* genes by bisulfite sequencing and their respective transcriptional increase by qPCR. We speculate that changes in these 2 glutamate receptor genes may be directly regulated by DNMT3A reduction in the stressed brain and participate the physiological and behavioral response, since Glud2 has been shown to promote AMPA receptor GluR2 endocytosis (Hirai et al. 2003; Kohda et al. 2013a). This finding therefore provides a hint to connect the DNA methylation change and AMPA receptor dysfunction in our stress model.

We also found that the vast majority of DNA methylation changes disproportionally exists in nonpromoter regions, such as intergenic regions and introns. Although promoter methylation normally silences gene expression, the exact role of methylation in other regions has emerged to be important. Noncoding DNA sequences that account for over 95% of the genome are known to have regulatory roles on gene transcription. We hypothesize that DNA methylation may participate in this process as well. Moreover, though DNA methylation was known to occur mostly at CpG sites, accumulating evidence indicates non-CpG methylations (CpH, H = A/C/T) in neurons (Lister et al. 2013; Guo et al. 2014), and Dnmt3a is required for its establishment during early neural development (Stroud et al. 2017). Note that the RRBS assay has a preference to CpG-rich regions, so the DNA methylation dataset we generated is not ideal for a non-CpG

methylation analysis. It will be important to carry out whole genome DNA methylation profiling with single-base resolution to examine each cytosine's methylation status in the future.

In summary, we found that rats exposed to chronic stress exhibited a reduction of Dnmt3a in the PFC. Manipulations of Dnmt3a in PFC indicated its functional roles in neurotransmission and stress-related behaviors. Moreover, we also found that genome-wide DNA methylation changes in PFC of stressed rats were selectively clustered in multiple neuronal pathways, many of which were also enriched in transcriptome alterations.

## Supplementary Material

Supplementary material can be found at *Cerebral Cortex* online.

## Notes

We thank Xiaoqing Chen and Kaijie Ma for their excellent technical support. *Conflict of Interest*: The authors declare no conflict of interest.

## Funding

## Data Access

All RRBS and RNAseq data have been deposited into NCBI database (GEO ID: GSE147847).

## References

Akalin A, Kormaksson M, Li S, Garrett-Bakelman FE, Figueroa ME, Melnick A, Mason CE. 2012. methylKit: a comprehensive R package for the analysis of genome-wide DNA methylation profiles. *Genome Biol*. 13:R87.

Arnsten AF. 2009. Stress signalling pathways that impair prefrontal cortex structure and function. *Nat Rev Neurosci*. 10:410–422.

Bagot RC, Cates HM, Purushothaman I, Lorsch ZS, Walker DM, Wang J, Huang X, Schlüter OM, Maze I, Peña CJ, et al. 2016. Circuit-wide transcriptional profiling reveals brain region-specific gene networks regulating depression susceptibility. *Neuron*. 90:969–983.

Barker GR, Bird F, Alexander V, Warburton EC. 2007. Recognition memory for objects, place, and temporal order: a disconnection analysis of the role of the medial prefrontal cortex and perirhinal cortex. *J Neurosci*. 27:2948–2957.

Bolger AM, Lohse M, Usadel B. 2014. Trimmomatic: a flexible trimmer for Illumina sequence data. *Bioinformatics*. 30(15):2114–2120.

Day JJ, Sweatt JD. 2011. Epigenetic mechanisms in cognition. *Neuron*. 70:813–829.

de Kloet ER, Joëls M, Holsboer F. 2005. Stress and the brain: from adaptation to disease. *Nat Rev Neurosci*. 6:463–475.

D'Esposito M, Detre JA, Alsop DC, Shin RK, Atlas S, Grossman M. 1995. The neural basis of the central executive system of working memory. *Nature*. 378:279–281.

Dias C, Feng J, Sun H, Shao NY, Mazei-Robison MS, Damez-Werno D, Scobie K, Bagot R, LaBonté B, Ribeiro E, et al. 2014. β-catenin mediates stress resilience through Dicer1/microRNA regulation. *Nature*. 516:51–55.

Dulac C. 2010. Brain function and chromatin plasticity. *Nature*. 465:728–735.

Duric V, Banasr M, Licznerski P, Schmidt HD, Stockmeier CA, Simen AA, Newton SS, Duman RS. 2010. A negative regulator of MAP kinase causes depressive behavior. *Nat Med*. 16:1328–1332.

Durinck S, Spellman PT, Birney E, Huber W. 2009. Mapping identifiers for the integration of genomic datasets with the R/Bioconductor package biomaRt. *Nat Protoc*. 4:1184–1191.

Elliott E, Manashirov S, Zwang R, Gil S, Tsoory M, Shemesh Y, Chen A. 2016. Dnmt3a in the medial prefrontal cortex regulates anxiety-like behavior in adult mice. *J Neurosci*. 36:730–740.

Feng J, Chang H, Li E, Fan G. 2005. Dynamic expression of de novo DNA methyltransferases Dnmt3a and Dnmt3b in the central nervous system. *J Neurosci Res*. 79:734–746.

Feng J, Pena CJ, Purushothaman I, Engmann O, Walker D, Brown AN, Issler O, Doyle M, Harrigan E, Mouzon E, et al. 2017. Tet1 in nucleus accumbens opposes depression- and anxiety-like behaviors. *Neuropsychopharmacology*. 42:1657–1669.

Feng J, Zhou Y, Campbell SL, Le T, Li E, Sweatt JD, Silva AJ, Fan G. 2010. Dnmt1 and Dnmt3a maintain DNA methylation and regulate synaptic function in adult forebrain neurons. *Nat Neurosci*. 13:423–430.

Fink DJ, DeLuca NA, Goins WF, Glorioso JC. 1996. Gene transfer to neurons using herpes simplex virus-based vectors. *Annu Rev Neurosci*. 19:265–287.

Fiori LM, Turecki G. 2011. Epigenetic regulation of spermidine/spermine N1-acetyltransferase (SAT1) in suicide. *J Psychiatr Res*. 45:1229–1235.

Gispen-de Wied CC. 2000. Stress in schizophrenia: an integrative view. *Eur J Pharmacol*. 405:375–384.

Goldman-Rakic PS. 1995. Cellular basis of working memory. *Neuron*. 14:477–485.

Guo JU, Su Y, Shin JH, Shin J, Li H, Xie B, Zhong C, Hu S, Le T, Fan G, et al. 2014. Distribution, recognition and regulation of non-CpG methylation in the adult mammalian brain. *Nat Neurosci*. 17:215–222.

Haller J, Harold G, Sandi C, Neumann ID. 2014. Effects of adverse early-life events on aggression and anti-social behaviours in animals and humans. *J Neuroendocrinol*. 26:724–738.

Heim C, Nemeroff CB. 2001. The role of childhood trauma in the neurobiology of mood and anxiety disorders: preclinical and clinical studies. *Biol Psychiatry*. 49:1023–1039.

Heinz S, Benner C, Spann N, Bertolino E, Lin YC, Laslo P, Cheng JX, Murre C, Singh H, Glass CK. 2010. Simple combinations of lineage-determining transcription factors prime cis-regulatory elements required for macrophage and B cell identities. *Mol Cell*. 38:576–589.

Hirai H, Launey T, Mikawa S, Torashima T, Yanagihara D, Kasaura T, Miyamoto A, Yuzaki M. 2003. New role of δ2-glutamte receptors in AMPA receptor trafficking and cerebellar function. *Nat Neurosci*. 6(8):849–876.

Kanehisa M, Sato Y, Furumichi M, Morishima K, Tanabe M. 2019. New approach for understanding genome variations in KEGG. *Nucleic Acids Res*. 47(D1):D590–D595.

Kohda K, Kategawa W, Matsuda S, Yamamoto T, Hirano H, Yuzaki M. 2013a. The δ2 glutamate receptor gates long-term depression by coordinating interactions between two AMPA receptor phosphorylation sites. *PNAS*. 110(10): E948–E957.

Kohda K, Kategawa W, Yuzaki M. 2013b. Unlocking the secrets of the δ2 glutamate receptor. *Communicative & Integrative Biology*. 6:6.e26466-1–e26466-3.

Kim D, Paggi JM, Park C, Bennett C, Salzberg SL. 2019. Graph-based genome alignment and genotyping with HISAT2 and HISAT-genotype. *Nat Biotechnol*. 37(8):907–915.

Kang HJ, Kim JM, Lee JY, Kim SY, Bae KY, Kim SW, Shin IS, Kim HR, Shin MG, Yoon JS. 2013. BDNF promoter methylation and suicidal behavior in depressive patients. *J Affect Disord*. 151:679–685.

Kim JM, Stewart R, Kang HJ, Kim SW, Shin IS, Kim HR, Shin MG, Kim JT, Park MS, Cho KH, et al. 2013. A longitudinal study of SLC6A4 DNA promoter methylation and poststroke depression. *J Psychiatr Res*. 47:1222–1227.

Klengel T, Mehta D, Anacker C, Rex-Haffner M, Pruessner JC, Pariante CM, Pace TW, Mercer KB, Mayberg HS, Bradley B, et al. 2013. Allele-specific FKBP5 DNA demethylation mediates gene-childhood trauma interactions. *Nat Neurosci*. 16:33–41.

Klengel T, Pape J, Binder EB, Mehta D. 2014. The role of DNA methylation in stress-related psychiatric disorders. *Neuropharmacology*. 80:115–132.

Krueger F, Andrews SR. 2011. Bismark: a flexible aligner and methylation caller for Bisulfite-Seq applications. *Bioinformatics*. 27:1571–1572.

Labonté B, Suderman M, Maussion G, Navaro L, Yerko V, Mahar I, Bureau A, Mechawar N, Szyf M, Meaney MJ, et al. 2012. Genome-wide epigenetic regulation by early-life trauma. *Arch Gen Psychiatry*. 69:722–731.

LaPlant Q, Vialou V, Covington HE 3rd, Dumitriu D, Feng J, Warren BL, Maze I, Dietz DM, Watts EL, Iñiguez SD, et al. 2010. Dnmt3a regulates emotional behavior and spine plasticity in the nucleus accumbens. *Nat Neurosci*. 13:1137–1143.

Levenson JM, Roth TL, Lubin FD, Miller CA, Huang IC, Desai P, Malone LM, Sweatt JD. 2006. Evidence that DNA (cytosine-5) methyltransferase regulates synaptic plasticity in the hippocampus. *J Biol Chem*. 281:15763–15773.

Li H, Handsaker B, Wysoker A, Fennell T, Ruan J, Homer N, Marth G, Abecasis G, Durbin R, 1000 Genome Project Data Processing Subgroup. 2009. The Sequence Alignment/Map format and SAMtools. *Bioinformatics*. 25:2078–2079.

Liao Y, Smyth GK, Shi W. 2014. featureCounts: an efficient general purpose program for assigning sequence reads to genomic features. *Bioinformatics*. 30(7):923–930.

Linhart HG, Lin H, Yamada Y, Moran E, Steine EJ, Gokhale S, Lo G, Cantu E, Ehrich M, He T, et al. 2007. Dnmt3b promotes tumorigenesis in vivo by gene-specific de novo methylation and transcriptional silencing. *Genes Dev*. 21:3110–3122.

Lister R, Mukamel EA, Nery JR, Urich M, Puddifoot CA, Johnson ND, Lucero J, Huang Y, Dwork AJ, Schultz MD, et al. 2013. Global epigenomic reconfiguration during mammalian brain development. *Science*. 341:1237905.

Lupien SJ, McEwen BS, Gunnar MR, Heim C. 2009. Effects of stress throughout the lifespan on the brain, behaviour and cognition. *Nat Rev Neurosci*. 10:434–445.

Maeng LY, Shors TJ. 2013. The stressed female brain: neuronal activity in the prelimbic but not infralimbic region of the medial prefrontal cortex suppresses learning after acute stress. *Front Neural Circuits*. 7:198.

Márquez C, Poirier GL, Cordero MI, Larsen MH, Groner A, Marquis J, Magistretti PJ, Trono D, Sandi C. 2013. Peripuberty stress leads to abnormal aggression, altered amygdala and orbitofrontal reactivity and increased prefrontal MAOA gene expression. *Transl Psychiatry*. 3:e216.

McEwen BS, Morrison JH. 2013. The brain on stress: vulnerability and plasticity of the prefrontal cortex over the life course. *Neuron*. 79:16–29.

McGowan PO, Sasaki A, D'Alessio AC, Dymov S, Labonté B, Szyf M, Turecki G, Meaney MJ. 2009. Epigenetic regulation of the glucocorticoid receptor in human brain associates with childhood abuse. *Nat Neurosci*. 12:342–348.

Meissner A, Gnirke A, Bell GW, Ramsahoye B, Lander ES, Jaenisch R. 2005. Reduced representation bisulfite sequencing for comparative high-resolution DNA methylation analysis. *Nucleic Acids Res*. 33:5868–5877.

Miller CA, Gavin CF, White JA, Parrish RR, Honasoge A, Yancey CR, Rivera IM, Rubio MD, Rumbaugh G, Sweatt JD. 2010. Cortical DNA methylation maintains remote memory. *Nat Neurosci*. 13:664–666.

Miller CA, Sweatt JD. 2007. Covalent modification of DNA regulates memory formation. *Neuron*. 53:857–869.

Miller EK, Cohen JD. 2001. An integrative theory of prefrontal cortex function. *Annu Rev Neurosci*. 24:167–202.

Mineur YS, Belzung C, Crusio WE. 2006. Effects of unpredictable chronic mild stress on anxiety and depression-like behavior in mice. *Behav Brain Res*. 175:43–50.

Morris MJ, Monteggia LM. 2014. Role of DNA methylation and the DNA methyltransferases in learning and memory. *Dialogues Clin Neurosci*. 16:359–371.

Muñoz P, Estay C, Díaz P, Elgueta C, Ardiles ÁO, Lizana PA. 2016. Inhibition of DNA methylation impairs synaptic plasticity during an early time window in rats. *Neural Plast*. 2016:4783836.

Nelson ED, Kavalali ET, Monteggia LM. 2008. Activity-dependent suppression of miniature neurotransmission through the regulation of DNA methylation. *J Neurosci*. 28:395–406.

Niwa M, Jaaro-Peled H, Tankou S, Seshadri S, Hikida T, Matsumoto Y, Cascella NG, Kano S, Ozaki N, Nabeshima T, et al. 2013. Adolescent stress-induced epigenetic control of dopaminergic neurons via glucocorticoids. *Science*. 339:335–339.

Paus T, Keshavan M, Giedd JN. 2008. Why do many psychiatric disorders emerge during adolescence? *Nat Rev Neurosci*. 9:947–957.

Piggott VM, Bosse KE, Lisieski MJ, Strader JA, Stanley JA, Conti AC, Ghoddoussi F, Perrine SA. 2019. Single-prolonged stress impairs prefrontal cortex control of amygdala and striatum in rats. *Front Behav Neurosci*. 13:18.

Popoli M, Yan Z, McEwen BS, Sanacora G. 2011. The stressed synapse: the impact of stress and glucocorticoids on glutamate transmission. *Nat Rev Neurosci*. 13:22–37.

Qin L, Liu W, Ma K, Wei J, Zhong P, Cho K, Yan Z. 2016. The ADHD-linked human dopamine D4 receptor variant D4.7 induces over-suppression of NMDA receptor function in prefrontal cortex. *Neurobiol Dis*. 95:194–203.

Radley JJ, Rocher AB, Janssen WG, Hof PR, McEwen BS, Morrison JH. 2005. Reversibility of apical dendritic retraction in the rat medial prefrontal cortex following repeated stress. *Exp Neurol*. 196:199–203.

Radley JJ, Rocher AB, Miller M, Janssen WG, Liston C, Hof PR, McEwen BS, Morrison JH. 2006. Repeated stress induces dendritic spine loss in the rat medial prefrontal cortex. *Cereb Cortex*. 16:313–320.

Radley JJ, Rocher AB, Rodriguez A, Ehlenberger DB, Dammann M, McEwen BS, Morrison JH, Wearne SL, Hof PR. 2008. Repeated stress alters dendritic spine morphology in the rat medial prefrontal cortex. *J Comp Neurol*. 507:1141–1150.

Rainer G, Asaad WF, Miller EK. 1998. Selective representation of relevant information by neurons in the primate prefrontal cortex. *Nature*. 393:577–579.

Ito R, Nakano T, Hojo Y, Hashizume M, Koshiba M, Murakoshi T. 2020. Chronic restraint stress affects network oscillations in the anterior cingulate cortex in mice. *Neuroscience*. 437:172–183.

Ritchie ME, Phipson B, Wu D, Hu Y, Law CW, Shi W, Smyth GK. 2015. limma powers differential expression analyses for RNA-sequencing and microarray studies. *Nucleic Acids Res*. 43:e47.

Robinson MD, McCarthy DJ, Smyth GK. 2010. edgeR: a bioconductor package for differential expression analysis of digital gene expression data. *Bioinformatics*. 26(1):139–140.

Robinson MD, Oshlack A. 2010. A scaling normalization method for differential expression analysis of RNA-seq data. *Genome Biol*. 11(3):R25.

Yoshida S, Ohnishi R, Tsuneoka Y, Yamamoto-Mimura Y, Muramatsu R, Kato T, Funato H, Kuroda KO. 2018. Corticotropin-releasing factor receptor 1 in the anterior cingulate cortex mediates maternal absence-induced attenuation of transport response in mouse pups. *Front Cell Neurosci*. 12:204.

Shin J, Ming GL, Song H. 2014. DNA modifications in the mammalian brain. *Philos Trans R Soc Lond B Biol Sci*. 369(1652):20130512.

Smith JW, Seckl JR, Evans AT, Costall B, Smythe JW. 2004. Gestational stress induces post-partum depression-like behaviour and alters maternal care in rats. *Psychoneuroendocrinology*. 29:227–244.

Stankiewicz AM, Swiergiel AH, Lisowski P. 2013. Epigenetics of stress adaptations in the brain. *Brain Res Bull*. 98:76–92.

Stedenfeld KA, Clinton SM, Kerman IA, Akil H, Watson SJ, Sved AF. 2011. Novelty-seeking behavior predicts vulnerability in a rodent model of depression. *Physiol Behav*. 103:210–216.

Steiger H, Labonté B, Groleau P, Turecki G, Israel M. 2013. Methylation of the glucocorticoid receptor gene promoter in bulimic women: associations with borderline personality disorder, suicidality, and exposure to childhood abuse. *Int J Eat Disord*. 46:246–255.

Stroud H, Su SC, Hrvatin S, Greben AW, Renthal W, Boxer LD, Nagy MA, Hochbaum DR, Kinde B, Gabel HW, et al. 2017. Early-life gene expression in neurons modulates lasting epigenetic states. *Cell*. 171:1151–1164.e16.

Sultan FA, Day JJ. 2011. Epigenetic mechanisms in memory and synaptic function. *Epigenomics*. 3:157–181.

Tahiliani M, Koh KP, Shen Y, Pastor WA, Bandukwala H, Brudno Y, Agarwal S, Iyer LM, Liu DR, Aravind L, et al. 2009. Conversion of 5-methylcytosine to 5-hydroxymethylcytosine in mammalian DNA by MLL partner TET1. *Science*. 324:930–935.

Toth M, Halasz J, Mikics E, Barsy B, Haller J. 2008. Early social deprivation induces disturbed social communication and violent aggression in adulthood. *Behav Neurosci*. 122:849–854.

Turecki G, Meaney MJ. 2016. Effects of the social environment and stress on glucocorticoid receptor gene methylation: a systematic review. *Biol Psychiatry*. 79:87–96.

Ursini G, Bollati V, Fazio L, Porcelli A, Iacovelli L, Catalani A, Sinibaldi L, Gelao B, Romano R, Rampino A, et al. 2011. Stress-related methylation of the catechol-O-methyltransferase Val 158 allele predicts human prefrontal cognition and activity. *J Neurosci*. 31:6692–6698.

Veenema AH, Blume A, Niederle D, Buwalda B, Neumann ID. 2006. Effects of early life stress on adult male aggression and hypothalamic vasopressin and serotonin. *Eur J Neurosci*. 24:1711–1720.

Vinkers CH, Kalafateli AL, Rutten BP, Kas MJ, Kaminsky Z, Turner JD, Boks MP. 2015. Traumatic stress and human DNA methylation: a critical review. *Epigenomics*. 7:593–608.

Wang HQ, Tuominen LK, Tsai CJ. 2011. SLIM: a sliding linear model for estimating the proportion of true null hypotheses in datasets with dependence structures. *Bioinformatics*. 27(2):225–231.

Wankerl M, Miller R, Kirschbaum C, Hennig J, Stalder T, Alexander N. 2014. Effects of genetic and early environmental risk factors for depression on serotonin transporter expression and methylation profiles. *Transl Psychiatry*. 4: e402.

Wei J, Xiong Z, Lee JB, Cheng J, Duffney LJ, Matas E, Yan Z. 2016. Histone modification of Nedd4 ubiquitin ligase controls the loss of AMPA receptors and cognitive impairment induced by repeated stress. *J Neurosci*. 36:2119–2130.

Wei J, Yuen EY, Liu W, Li X, Zhong P, Karatsoreos IN, McEwen BS, Yan Z. 2014. Estrogen protects against the detrimental effects of repeated stress on glutamatergic transmission and cognition. *Mol Psychiatry*. 19:588–598.

Wilber AA, Walker AG, Southwood CJ, Farrell MR, Lin GL, Rebec GV, Wellman CL. 2011. Chronic stress alters neural activity in medial prefrontal cortex during retrieval of extinction. *Neuroscience*. 174:115–131.

Wilkinson MB, Dias C, Magida J, Mazei-Robison M, Lobo M, Kennedy P, Dietz D, Covington H 3rd, Russo S, Neve R, et al. 2011. A novel role of the WNT-dishevelled-GSK3$\beta$ signaling cascade in the mouse nucleus accumbens in a social defeat model of depression. *J Neurosci*. 31:9084–9092.

Xi Y, Li W. 2009. BSMAP: whole genome bisulfite sequence MAPping program. *BMC Bioinformatics*. 10:232.

Yu NK, Baek SH, Kaang BK. 2011. DNA methylation-mediated control of learning and memory. *Mol Brain*. 4:5.

Yuen EY, Wei J, Liu W, Zhong P, Li X, Yan Z. 2012. Repeated stress causes cognitive impairment by suppressing glutamate receptor expression and function in prefrontal cortex. *Neuron*. 73:962–977.